Welfare and Production Implications of Climate Change-Induced Impacts in Labour Capacity: Assessment warming to 2100 from 30 CMIP5 Earth System Models.

David Newth. *CSIRO Oceans and Atmosphere Flagship. The Commonwealth Scientific and Industrial Research Organisation. Canberra. Australia.*

Ernesto Valenzuela. *Faculty of Business. Federation University. Gippsland. Australia.*

Yiyong Cai. *CSIRO Oceans and Atmosphere Flagship. The Commonwealth Scientific and Industrial Research Organisation. Canberra. Australia.*

Don Gunasekera. *Institute for Supply Chain and Logistics, Victoria University. Melbourne. Australia.*

Abstract. Temperature and humidity are key factors that limit human activity particularly in tropical and mid-latitudes. Greenhouse-gas-induced warming shows an increase in absolute humidity, and this has implications for the capacity and productivity of the labour force to undertake and sustain economic activities. One metric that captures the impact of heat stress on the labour force is the wet-bulb globe temperature (WBGT). Here we use the WBGT to estimate the potential effect of climate change driven labour capacity changes under the alternative Representative Concentration Pathways (RCPs) 8.5, 6.0, 4.5 and 2.6 scenarios for a cross section of the CMIP5 model outputs. These labour capacity changes are then implemented as shocks to labour productivity within the GTAP model. The economy wide analysis of the impacts of future climate on labour force productivity suggests a labour capacity reduction to less than 30% under RCP8.5, in some regions of the world in 2100, leading to substantial medium to long term economic and welfare changes. The other RCP scenarios show that such dramatic changes in labour capacity can be avoided. The analysis here highlights the need for early mitigation and adaptation using appropriate technologies related to specific economic activities including relevant occupational health and safety measures.

1. Introduction

Humans are now the main cause of increased levels of greenhouse gases in the Earth's atmosphere (IPCC 2007). Projections from the latest generation of climate and Earth system models show that global surface air temperature will increase substantially in the future due to the radiative effects of the increased greenhouse gas concentrations (reference). Apart from surface air temperature, increased radiative effects will also increase absolute humidity (Manabe and Wetherald 1974). Idealized climate model experiments, using a 1% yr^{-1} increase in CO_2, have shown that various regions of the world, including Southeast Asia, southern USA, and northern Australia are particularly vulnerable to increases in surface air temperature and humidity (ref).

The combined effect of increased surface air temperature and humidity pose a significant threat to human health and wellbeing, in the form of heat stress. Various meteorological metrics have been developed to assess the impact of increase air temperature on human health. Of these metrics, the Wet Bulb Globe Temperature (WBGT) captures the combined effects of temperature and humidity, and has become the accepted international standard that provides a simple method for the assessment of hot environments (Parsons 2006). It is the intent of this paper to examine the changes in global and regional wet bulb globe temperature patterns, simulated by latest generation of earth system models in response to alternative GHG emissions pathways. The results illustrate the important extra burden that increased surface air temperature and humidity may place on human comfort as a consequence of climate change.

Heat indexes are measures of the stress placed on humans by elevated levels of atmospheric temperature and moisture. As the atmospheric moisture content increases the ability of the human body to relates head through evaporation is inhibited thereby causing discomfort and stress. The Wet Bulb Globe Temperature (WBGT) is an index that takes into account both surface air temperature and humidity, and is used across the world to control heat stress in many contexts including military, industrial, domestic, sporting and commercial settings.

The WBGT is also used in national (e.g. (UK, China, Japan, USA and Australia and international (ISO) standards. The ISO 7243 'Hot environments – Estimation of the heat stress on working man, based on the WGBT-index is accepted internationally as the standard that provides a simple method for assessment and control of heat stress in working environments.

The purpose of this paper is to explore the relationship between heat stress, labour capacity and the economic implications of increased heat stress. The rest of this paper is organised as follows. In Section 2 we defined how the WBGT is calculate from surface measurements. Section 2 concludes with a discussion on how WBGT index is used as a guide for safe labour capacity guidelines. Following on from this section 3 outlines the current generation of the IPCC global climate scenarios, the Representative Concentration Pathways (RCPs) and outlines the air surface temperature and WBGT changes associated with the four RCPs. Section 4, outlines the model configuration and experimental structure used to examine the impact of decreased labour capacity on economic productivity. Section 5 presents the main results from the proposed experiments. Finally section 6 provides a discussion of the results and present a number of key findings.

2. Heat Stress Metrics

Over the last century agronomists, physiologists and bio-meteorologists have attempted to develop environmental indices and metric that can be used as guidelines for human performance in hot environments. The WBGT index was proposed in order to avoid the elaborate producers of determine the Effective Temperature Index (ET), which was an empirical index derived from a series of laboratory studies around the 1920's that became the established method used to evaluate heat stress. The WBGT index combines temperature, humidity, radiation and wind into a single value which could be used for assessment of heat stress in a workplace. In the remainder of this section, we will present the Davis-Jones method, as presented by Dunne *et al*. 2013, for the calculation of WBGT from surface air temperature, surface humidity and pressure fields. Following on from this, we will present the ISO standard for maintaining safe labour capacity.

2.1 Calculation of Wet Bulb Globe Temperature from Observations

The WBGT is the accepted international standard that provides a simple method for the assessment of hot environments (Parsons 2006). The general from of the WBGT is:

$$T_{wbgt} = 0.7T_{wbt} + 0.2T_g + 0.1T_a,$$

Where T_{wbt} the natural wet bulb temperature; T_g is the temperature of a 150mm diameter black globe; and T_a is the air temperature. For indoor or shaded environments, $T_g \approx T_a$, and we adopt this implied form (Epstein and Moran 2006) :

$$T_{wbgt} = 0.7T_{wbt} + 0.3T_g,$$

The generalized definition of globe temperature involves the radiative balance such as directed exposure to sunlight and indoor room effects we approximate globe temperature as dry bulb temperature: $T_g = T_{ref} - 273.15$. We follow Dune *et al.* (2013) and use the Davies-Jones (2007) method for calculating the Wet-Bulb Temperature, we will briefly cover the calculation in the remainder of this section. Here, T_{ref} is the absolute temperature (K) at a reference level of 2m; $\mathrm{rh}_{\mathrm{ref}}$ is the relative humidity at a reference level of 2m ($0.01\% \le rh_{ref} \le 100\%$); and p_{ref} is the surface pressure (mbar). T_{wbt} is calculated by:

$$T_{wbt} = 45.114 - 51489\left(\frac{\theta_E}{273.15}\right)^{-3.504},$$

The wet bulb temperature (T_{wbt}) is the temperature of a parcel of air if it were cooled to saturation (100% relative humidity) by the evaporation of water into it, with the latent heat being supplied by the parcel. It should be noted that $T_{wbt} \le T_g$. θ_E, is the equivalent potential temperature (K); the temperature a parcel of air would reach if it were continued to be adiabatically lifted to condense all water, and then lowered dry adiabatically to 1000 mbar see Bolton (1980) eqn 43:

$$\theta_E = T_{ref}\left(\frac{1000}{p}\right)^{0.2854(1-0.28\times10^{-3}w)} exp\left(\left(\frac{3.376}{T_L} - 0.00254\right) w(1 + 0.81 \times 10^{-3}w)\right),$$

T_L is the lifting condensation temperature (K); the temperature at which relative humidity would reach 100% upon abiatic lifting defined as:

$$T_L = \frac{1}{\left(T_{ref} - 55 - ln\left(\frac{rh_{ref}}{100}\right)/2840\right)} + 55,$$

and we define w, the mixing ratio (g kg^{-1}) to be:

$$w = \frac{rh_{ref}}{100} w_{sat},$$

w_{sat} is the saturation missing ratio (g/kg):

$$w_{sat} = 621.97\frac{e_{sat}}{p - e_{sat}}$$

and finally, e_{sat}:

$$e_{sat} = exp\left(-\frac{2991.2729}{T_{ref}^2} - \frac{6017.0128}{T_{ref}} + 18.87643854 - 0.028354721T_{ref} + 1.7838310 \times 10^{-7}T_{ref}^2 - 8.4150417 \times 10^{-10}T_{ref}^3 + 4.4412543 \times 10^{-13}T_{ref}^4 + 2.858487\, ln(T_{ref})\right)/100$$

Is saturation mixing ratio (g kg^{-1}) (Boyed eqn 9).

In the experiments presented here, we use monthly averages (see section 3.X). By doing this we ignore the radiative and daytime extreme components, and therefore our estimates reflective of a lower limit of WBGT in shaded and optimally sheltered daytime or otherwise night time conditions.

2.2 Metabolic Rate and Wet Bulb Globe Temperature

To quantify the projected implications for human activity, we draw on industrial and military guidelines on threshold limit values for safety in occupational labour. This metric is a guide for moderating labour during a typical 8-h work day to reduce the threat of hyperthermia and its effects. Threshold limits for the WBGT index is provided in ISO 7243 and similar guidelines are provided by American Conference of Governmental Industrial Hygienists (ACGIH) (ref). These guidelines differ in their threshold values for particular forms of labour. Regardless of the threshold levels, the guidelines take into account the amount of effort exerted while performing a given task (metabolic rate expressed in Wm^{-2}), and the WBGT. The relationship between work and rest, WBGT, and effort exerted is shown in figure X.

Following the ISO and ACGIH, we distinguish between three forms of labour. Light labour, an individual has a metabolic rate (M) of $M \leq 65Wm^{-2}$; Medium labour, an individual has a metabolic rate of $65 \leq M \leq 130Wm^{-2}$; and Heavy labour, an individual has a metabolic rate of $65 \leq M \leq 130Wm^{-2}$. Example of each of these classes of labour is given in Table X. For a continuous representation of labour capacity L (percentage of work to rest) across the thresholds we develop an algorithm for each category of labour.

$$L = 100 - C \max{(0, WBGT - C)}^{2/3} .$$

Where C is threshold value for continuous work for a given category of labour. This relationship is robust across all categories of work, and provides a systematic approach to the calculation of labour capacity.

3. Climate Projections and Representative Concentration Pathways

3.1 The Representative Concentration Pathways

The IPCC are making increased use of Integrated Assessment Models (IAM's) to study the environmental, economic and social consequences of action to mitigate climate change. For example, four IAMs were employed to each model one of the RCPs to ensure they are economically and biophysically feasible. These marker scenarios were provided for RCP2.6 by IMAGE (van Vuuren *et al*., 2011a); for RCP4.5 by GCAM (Thomson *et al.,* 2011); for RCP 6.0 by AIM (Masui et *al*. 2011) and for RCP 8.5 by MESSAGE (Riahi *et al*., 2011). The RCPs are defined as trajectories of globally averaged radiative forcing at the top of the atmosphere, culminating in values in 2100 of 2.6, 4.5, 6.0 and 8.5 Wm^{-2}, respectively above the forcing in the reference year, 1850. In principle, each RCP could be achieved by a wide range of emissions scenarios, representing different combinations of social, economic and technological settings. The four RCP marker simulations span a wide range of actions on climate change from RCP8.5, which is effectively a 'business as usual' scenario resulting in a climate warming of 3.2-5.4K by 2100, through to RCP2.6, a rapid and ambitious mitigation scenario that stabilizes warming at approximately 2K above preindustrial levels.

The 'business-as-usual' case, RCP8.5, results in an atmospheric CO_2 concentration of >1350ppm CO_2e in 2100. The two moderate action scenarios, RCP6.0 (Masui *et al*., 2011) and RCP4.5 (Thomson *et al.*, 2011) lead to atmospheric concentrations of ≈850ppm and ≈650ppm CO_2e respectively in 2100. The ambitious action RCP2.6 is a peak-and-decline scenario, where radiative forcing reaches ≈3 Wm^{-2} in 2060 and declines to ≈2.6 Wm^{-2} in 2100 with a corresponding concentration peak of ≈490ppm CO_2e. The CO_2 emissions trajectories, for each of the RCP marker scenarios are shown in Figure 1. RCP2.6 (van Vuuren *et al*., 2011a) scenario requires negative fossil fuel emissions after 2080 in order to achieve the target. The IMAGE modelling underpinning this scenario uses BECCS to achieve negative emissions.

At present, global emissions are tracking above the IPCC RCP8.5 scenario (Riahi *et al.*, 2011; Le Quere *et al.*, 2014). Should we continue to follow this emissions trajectory, we can expect an increase in surface air temperature of 3.2-5.4^{o}K by 2100. The disruptive impact of such climate changes will be severe and will disproportionally affect the poorest (IPCC 2014).

3.2 Climate Projections

Changes in wet bulb globe temperature associated with each RCP emission trajectory is base on the output of a multi-model ensemble of climate and earth system model simulations of history and RCP scenarios for 1860–2100, that were contributed to the Coupled Model Intercomparison Project Phase 5

(CMIP5) (ref). The models display a wide range climate sensitivities, with Equilibrium Climate Sensitivity (ECS) that range over 2.0-4.67 K, and Transitives Climate Response (TCR) that range over 1.1-2.5 K, allowing the analysis to explore a robust set of climate uncertainties (Forster et al. 2013). A list of models used in the study is given in Table 1, along with the RCPs scenarios used. Figure X, shows the relative change in global average surface air temperature averaged over the decade 2091-2100, compared to the long term average between 1860-2000. For RCP2.6, air surface temperature ranges of 0.8-2.2 K, with 17 of the modesl staying below 2 K; RCP 4.5 1.5-3.1 K, RCP6.0 2.1-3.7 K; and RCP8.5 3.3-5.7 K.

In order to assure that model results were consistent with instrument observations, each scenario used was corrected to the National Center for Environmental Prediction (NCEP) reanalysis (ref). We made two sets of correction based on comparisons of mean monthly WBGT. The first relates the bias in the mean geographic pattern in climatological mean WBGT and the second to biases in decadal scale variability on the positive extremes from the climatological mean.

The NCEP reanalysis period used in this study was for 1948–2013. To correct for model biases in the climatological mean, we calculate a monthly climatology for both model in question and NCEP and then took the difference between the maximum in each climatology to apply as an anomaly for a mean corrected WBGT. The correction for the model relative excesses in decadal scale variablity and resulting extremes was more involved. Over the NCEP reanalysis period of 1948-2013, there is considerable inter-annual variability as well as a long term trend. In order to isolate biases in variability on decala scale we binned the NCEP and model data into six decades (1951-1960, 1961-1970, 1971-1980, 1981-1990, 1991-2000, and 2001-2010. For each decade we calculate a monthly climatology. We then calculated the difference between the decal maximum and the climatological maximum for each decade. This gives six estimate of historical departure beyond the decal climatological maximum month, which we then averaged for a single decal-scale variability estimate for both NCEP (WBGT)NCEP_DMA) and Model_DMA, and then the decadal mean maximum WBGT(DM) as the 10 year boxcar smoothed vales of WBGT_AM (filling in the beginning and ending decades with median values for those decades). We then calculate the variance corrected WBDT (VC) as:

$$T_{wbgt}^{VC} = T_{wbgt}^{MC} - \left(T_{wbgt}^{AM} - T_{wbgt}^{DM}\right)\left(1 - \frac{T_{wbgt}^{NCEP\ DMA}}{T_{wbgt}^{Model\ DMA}}\right)$$

The variance correction is applied when WBGT_NCEP/WBGT_DMA is less than one in order to selectively reduce the model variability to levels of the NCEP and avoid adding variability where NCEP gave more variability than the model in question.

3.3 Global and Regional Changes in WBGT

Figures X and Y show the trajectory of average global change in WBGT from 1950-2100, relative to the long term average (1948-2010), and spatial patterns in the maximum monthly WBGT. For RCP2.6, global average WBGT increases between 0.6–1.7^{o}C (ensemble average of 1.1^{o}C); RCP 4.5 increases between 1.1-2.4^{o}C (ensemble average of 1.72^{o}C), RCP 6.0 increases between 1.6–2.8^{o}C (ensemble average of 2.1^{o}C); and RCP8.5 2.37-4.4^{o}C (ensemble average of 3.36^{o}C). The WBGT differ from surface air temperature, because of the effect humidity and potential evaporation.

The spatial patters of changes in WBGT are show in figure Y. Figure Y(a) show the maximum WBGT for the decade 1950-1960, while figure Y(b) shows the pattern for the most recent decade. Averaged over the ensemble of models. The results show a robust pattern of change in WBGT across the globe. The Middle East, Northern Africa, Pakistan and India, Northern South America, USA and Northern Australia will all experience a increases in WBGT that will significantly impede labour productivity.

4. Experiments

4.1 The GTAP Model

To estimate the impacts of reduced labour capacity shocks on welfare and production, we use the Global Trade Analysis Project (GTAP) general equilibrium global trade model and its accompanying database and recently developed poverty modules (Hertel, 1997; Dimaranan, 2006; Hertel et al., 2007). GTAP is a widely used, comparative static, general equilibrium model which tracks trade flows between all regions in the world, and explicitly models the consumption and production for all commodities of each national economy. Producers are assumed to maximize profits, while consumers maximize utility. Factor market clearing requires that supply equal demand for agricultural and non-agricultural skilled and unskilled labor and capital, natural resources and agricultural land, and adjustments in each of these markets in response to the climate change shocks determines the resulting wage and rental rate impacts. The model has recently been validated with respect to its performance in predicting the price impacts of exogenous supply side shocks, such as those that might result from global climate change (Valenzuela et al., 2007).

We divided the economy up into 30 regions and 20 commodities. The list of regions is given in Table 2.

4.1 Labour Capacity Shocks

Productivity shocks in labour supply due to climate change between 2007 and 2100 were calculated based on the CMIP5 results and labour capacity calculations presented in section 3. For each model results, a decadal climatology of labour capacity was calculated and then the labour capacity was taken as the mean of the climatologically monthly maximums. Each of the sectors was mapped into a category of labour intensity. Table 3, the three classes of labour intensity (heavy, medium and light), and the sectors that map into them. The Labour supply shock *S*, was calculated as:

$$S_I = 100 - L_I \, .$$

Where I, is the intensity of the labour. It should be noted that these shocks assume that individuals are adequately acclimatised to the environment and their attire is optimal for the climatic conditions in their region. Tables X-Z, shows the distribution of shocks across the ensemble of models for each geographical region for the historical simulation for the reference period and 2100 for each of the RCP warming scenarios. The Shock supplied to the GTAP model were calculated as:

$$S_I^{GTAP} = S_I^{RCP\,2100} - S_I^{Historical\,2010} \, .$$

For each model, RCP scenario and sector of the economy.

5. Results and Discussion

The results highlight the expected influence of the debilitating impact on labour across many regions in the world as simulated in this study. The decline in labour productivity due to climate warming will have several effects. First, it is estimated to reduce the production of many goods and services in adversely affected regions, and in particular in labour intensive industries such as agriculture and construction. When economic output falls so too does aggregate income, and all else being equal, less goods and service can be afforded, so consumptions falls as well.

The developing country share of global exports (imports) of many primary industry products such as agriculture is estimated to be lower (higher) over the projection period than in the absence of climate warming driven reduction in labour productivity.

Furthermore, decline in economic output in developing regions is estimated to lower their consumption and economic welfare relative to what would otherwise be. This trend is particularly remarkable in regions such as India, Pakistan, Bangladesh, Egypt and the Middle East. This highlights the fact that fall in labour productivity due to climate warming is non-trivial from a national, regional and global economic and welfare perspective. Unsurprisingly almost all of the global welfare loss is estimated to be felt by developing country regions.

International prices of primary and resource commodities are estimated to increase over time . This affects countries' terms of trade (and hence incomes) in different ways, depending on their net exports of the various products. Part of the reason for drop in consumption is the fall in household incomes in those countries where decline in labour productivity due to climate warming and rise in WBGTs is highest. Overall, economic welfare falls for those countries where drop in labour productivity is highest.

In contrast, countries in cooler or temperate regions are estimated to be affected far less economically. Since the changes in labour productivity are region specific, they will also impact long-term economic growth prospects and trade relations.

Overall trade would be expected to decline as global output declines. The re-shaping of international trade will depend on how the relative changes in labour productivity across different regions are reflected in competitiveness and prices. These impacts will vary substantially across sectors (for example, reflecting the relative labour intensity of output in different sectors) and across regions (reflecting both the product mix of output (industries) and labour intensity).

6. Conclusion

The Wet Bulb Globe Temperature is a measure of the stress placed on humans by increased surface air temperature and moisture. As the atmospheric moisture content increases the ability of the human body to release head through evaporation is inhibited, thereby causing discomfort and stress. Here we have analysed the changes in global patterns of WBGT and the associated shifts in labour capacity.

Overall, we show that consideration of the moist thermal response under climate warming poses increasingly sever environmental limitations on individual labour capacity as set by occupational standards in the coming decades specifically in lost labour capacity in peak months of heat stress, even if the global community commits to moderate action on mitigation climate change (RCP 6.0 and RCP 4.5). This reduction in labour capacity has significant implications for poverty and economic development. Under the highest scenario considered (RCP 8.5), mid latitude regions are vulnerable to reduced labour productivity. Emerging economies in the mid latitudes, such as Pakistan, Middle East, India, Northern Africa and Bangladesh, are particularly at vulnerable to environmental heat stress.

Acknowledgements

The authors would like to thank John Dunne for his help in performing the WBGT calculations.

References

Davies-Jones, R. (2007) An efficient and accurate method for computing the wet-bulb temperature along pseudoabiadats. *Monthly Weather Review*. vol 136. 2764–2785.

Dunne, J. P., Stauffer, R. J., and John, J. G. (2013) Reductions in labour capacity from heat stress under climate warming. *Nature Climate Change*. VOL. PP.

Epstein, Y. and Moran, D. S. (2006) Thermal comfort and the heat stress indices. *Industrial Health*. vol 44. 388–398.

Forster, P. M., Andrews, T., Good, P., Gregory, J. M., Jackson, L. S. and Zelinka, M. (2013) Evaluating adjusted forcing and model spread for historical and future scenarios in the CMIP5 generation of climate models. *Journal of Geophysical Research: Atmospheres*. vol 118. 1139-1150. DOI:10.1002/jgrd.50174

Taylor, K. W., Stouffer, R. J., and Meehl, G. (2012) An Overview of CMIP5 and the experiment design. American Meteorological Society. 485–498.

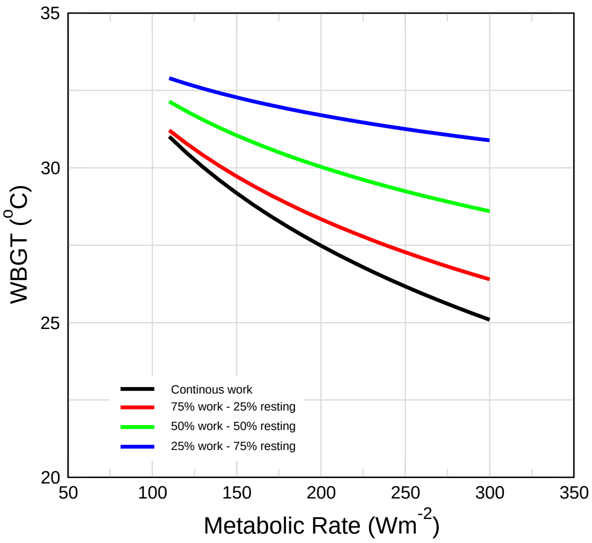

Figure X. Relationship between WBGT metabolic rate and Labour Capacity (redrawn from ISO7243). For a given metabolic rate and WBGT, the ratio of rest to labour can be calculated. While these are generic guidelines, they do provide a robust lower bound to maintaining safe working conditions.

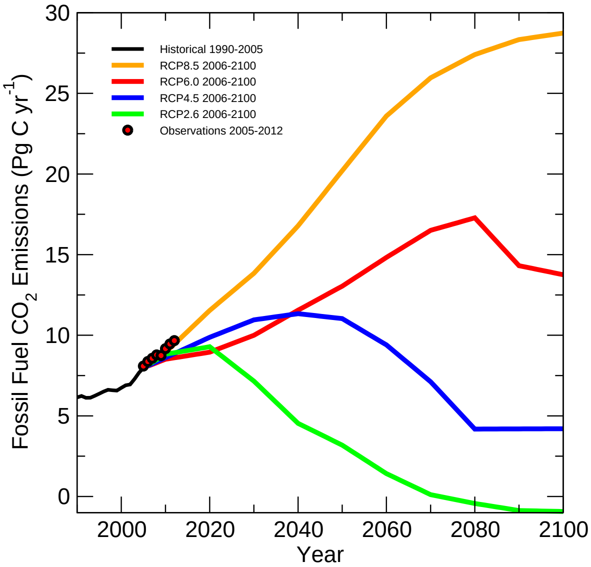

Figure X. The CO2 Emissions Pathways for the four IPCC RCP scenarios. Observations from the Global Carbon Project show that we are currently tracking above RCP8.5 scenario.

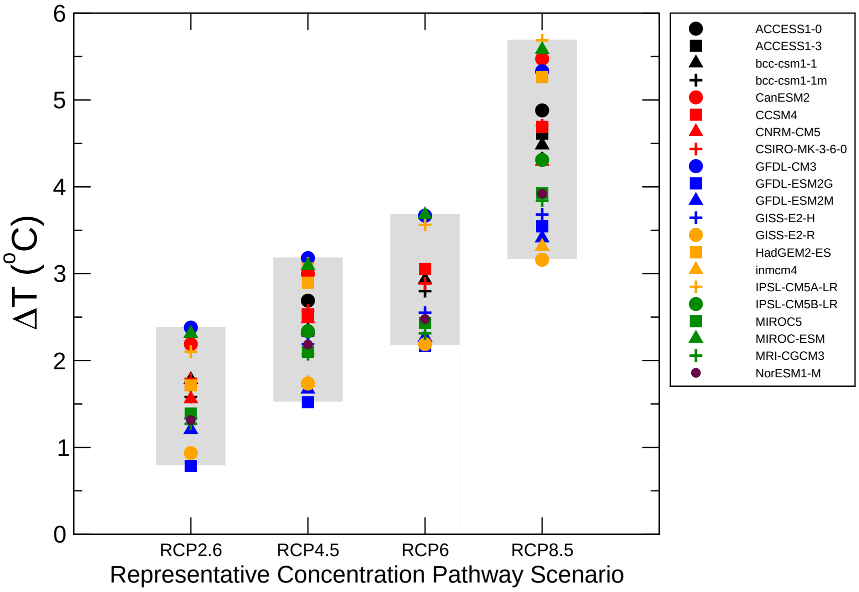

Figure 1. Changes in Global average Surface Air Temperature, averaged over the period 2091-2100, from the long term average global average surface air temperature 1860-2000, for the Global Climate Model and Earth Systems Models submitted to CMIP5 process. RCP2.6 <DELETE?>

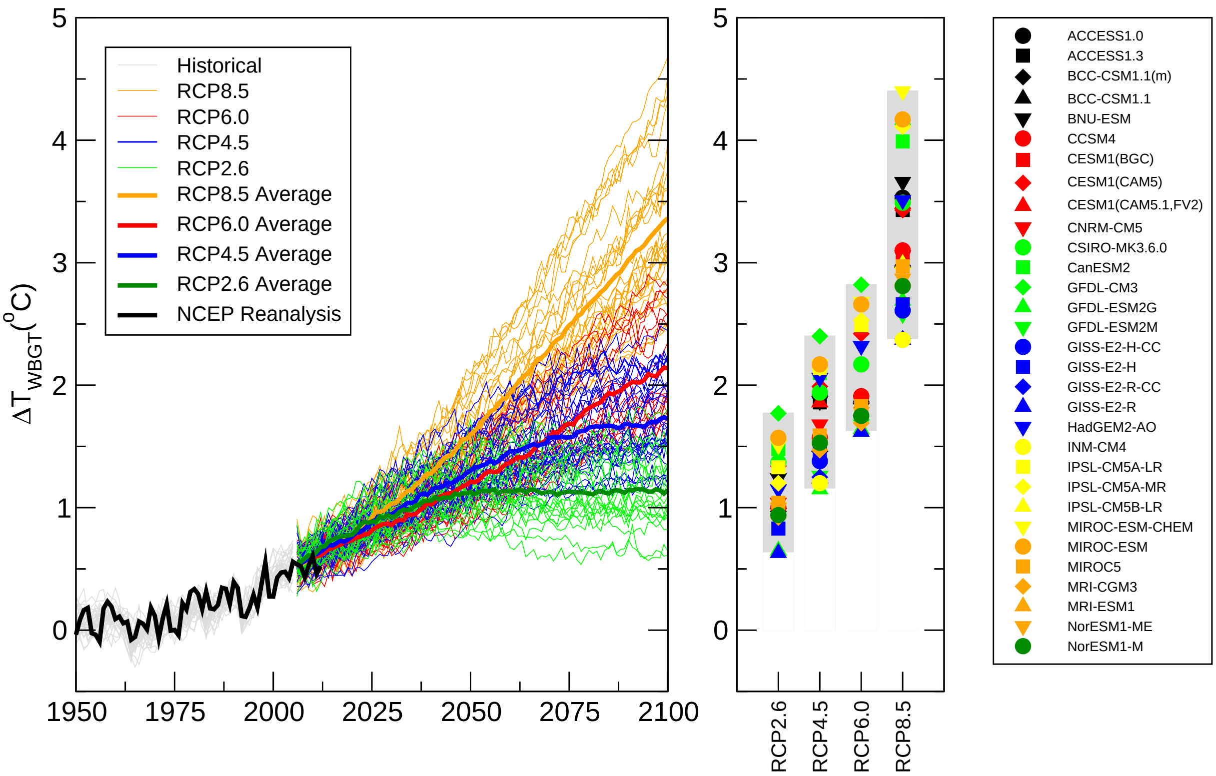

Figure X. Average global change in WBGT from 1950-2100, relative to the long term average (1948-2010), and spatial patterns in the maximum monthly WBGT. For RCP2.6, global average WBGT increases between 0.6–1.7°C (ensemble average of 1.1°C); RCP 4.5 increases between 1.1-2.4°C (ensemble average of 1.72°C), RCP 6.0 increases between 1.6–2.8°C (ensemble average of 2.1°C); and RCP8.5 2.37-4.4°C (ensemble average of 3.36°C).

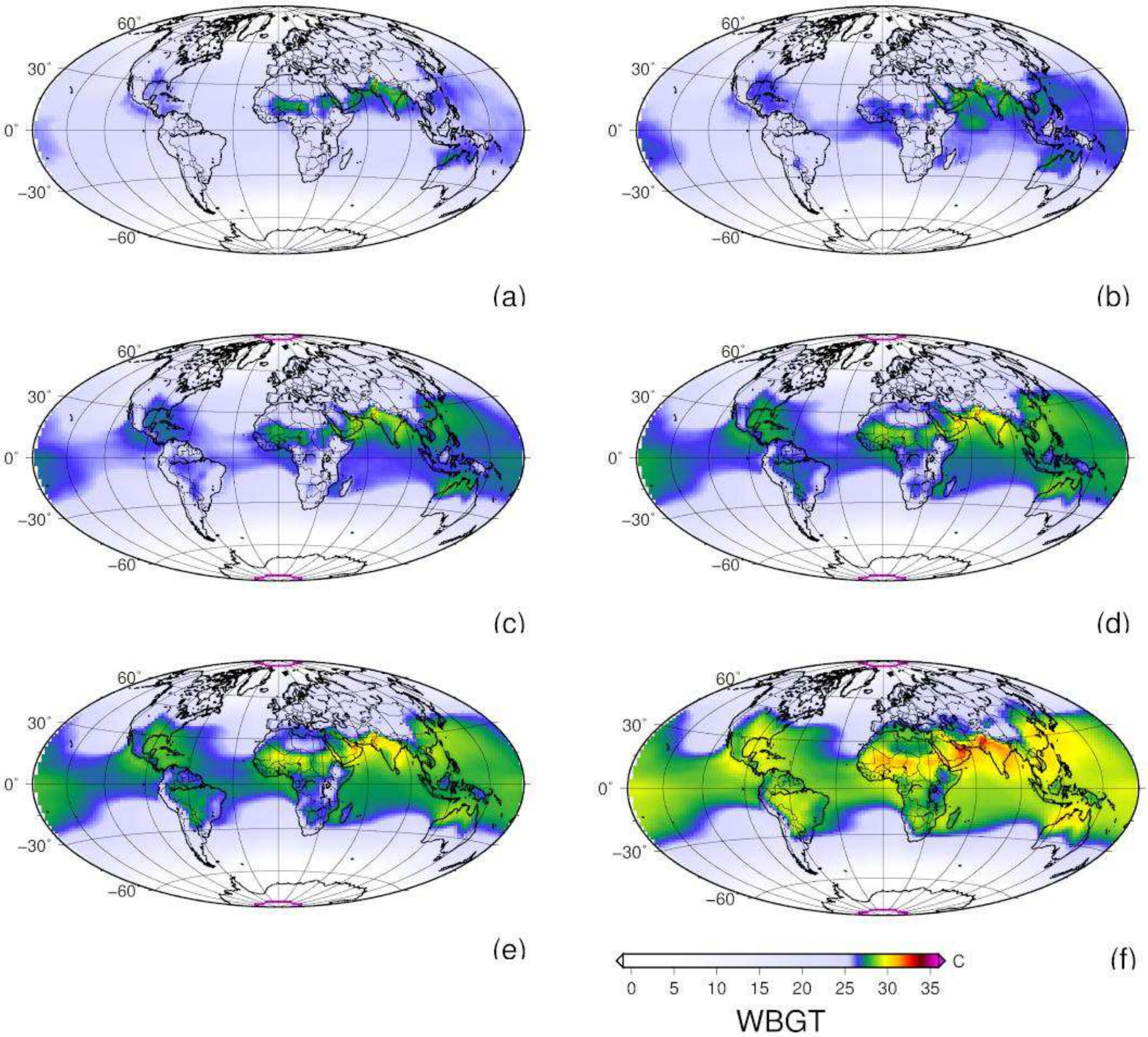

Figure X. Projected maximum monthly Wet Bulb Globe Temperature under the Representative Concentration Pathways. (a) NCEP reanalysis 1951-1960. (b) NCEP reanalysis for the most recent decade 2001-2010. (c) Projected maximum monthly WBGT for RCP 2.6 for 2091-2100 (d) Projected maximum monthly WBGT for RCP 4.5 for 2091-2100. (e) Projected maximum monthly WBGT for RCP 6.0 for 2091-2100; and (f) Projected maximum monthly WBGT for RCP 8.5 for 2091-2100. Each of the RCP projections is averaged over an ensemble of models from CMIP5 listed in Table X.

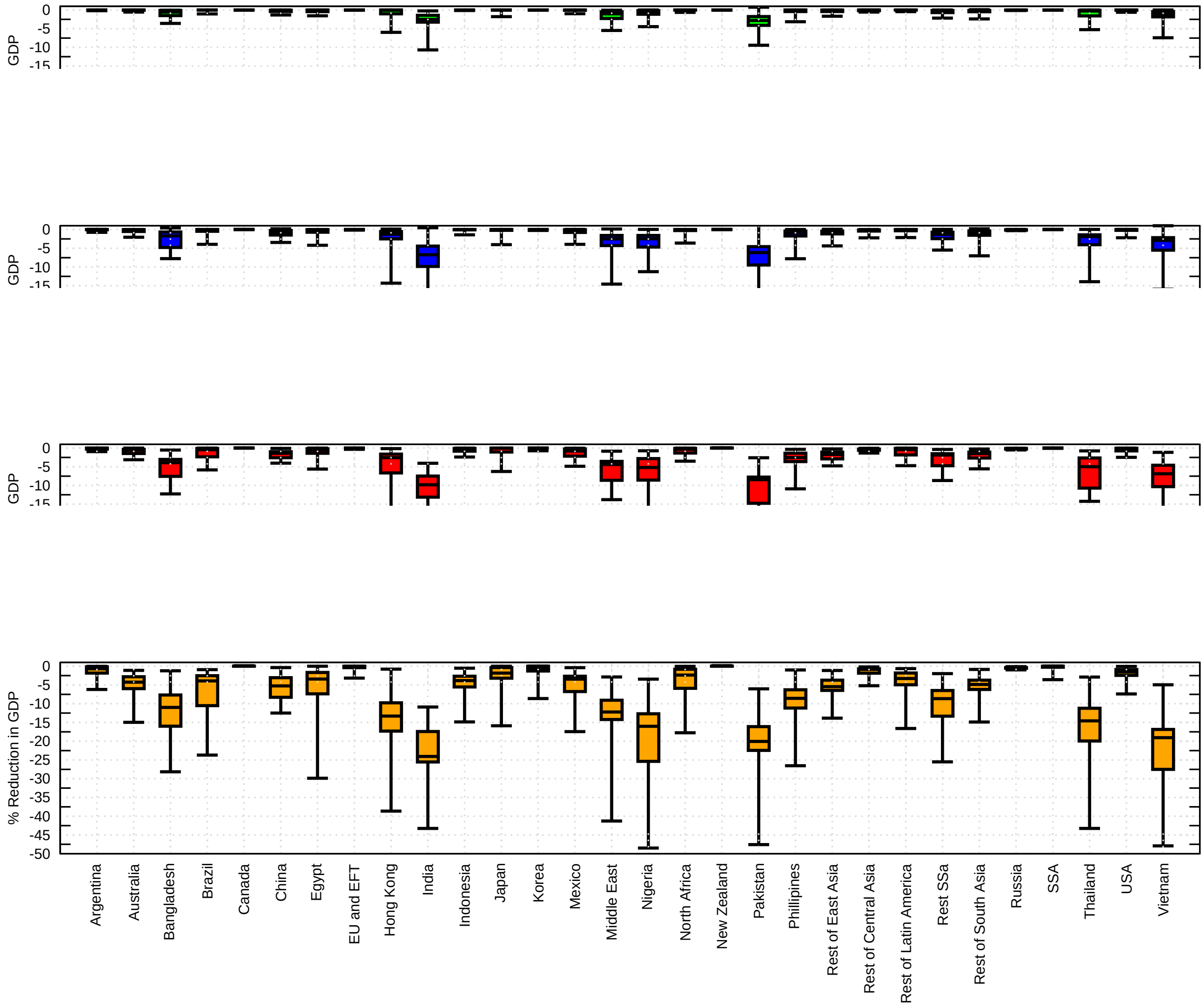
GDP
0
-5
-10
-15
GDP
0
-5
-10
-15
GDP
0
-5
-10
-15
% Reduction in GDP
0
-5
-10
-15
-20
-25
-30
-35
-40
-45
-50
Argentina
Australia
Bangladesh
Brazil
Canada
China
Egypt
EU and EFT
Hong Kong
India
Indonesia
Japan
Korea
Mexico
Middle East
Nigeria
North Africa
New Zealand
Pakistan
Phillipines
Rest of East Asia
Rest of Central Asia
Rest of Latin America
Rest SSa
Rest of South Asia
Russia
SSA
Thailand
USA
Vietnam

Table 1. Climate and Earth Systems Models used in this Study.

Model	RCP 2.6	RCP 4.5	RCP 6.0	RCP 8.5
ACCESS1.0		×		×
ACCESS1.3		×		×
BCC-CSM1.1(m)	×	×	×	×
BCC-CSM1.1	×	×	×	×
BNU-ESM	×	×		×
CanESM2	×	×		×
CCSM4	×	×	×	×
CESM1(CAM5.1,FV2)		×		×
CESM1(CAM5)	×	×	×	×
CNRM-CM5	×	×		×
CSIRO-Mk3.6.0	×	×	×	×
GFDL-CM3	×	×	×	×
GFDL-ESM2G	×	×	×	×
GFDL-ESM2M		×	×	×
GISS-E2-H-CC		×		×
GISS-E2-H	×	×	×	×
GISS-E2-R-CC		×		×
GISS-E2-R	×	×	×	×
HadGEM2-AO	×	×	×	×
INM-CM4		×		×
IPSL-CM5A-LR	×	×	×	×
IPSL-CM5A-MR	×	×	×	×
IPSL-CM5B-LR		×		×
MIROC5	×	×	×	×
MIROC-ESM-CHEM	×	×	×	×
MIROC-ESM	×	×	×	×
MRI-CGCM3	×	×	×	×
MRI-ESM1				×
NorESM1-ME	×	×	×	×
NorESM1-M	×	×	×	×

Table 1. Examples of Activities within Metabolic Rate Categories.

Region	Example Activities
Light	Sitting with moderate arm and leg movements. Standing with light work at machine or bench while using mostly arms. Using a table saw. Standing with light or moderate work at machine or bench and some walking about.
Moderate	Scrubbing in a standing position Walking about with moderate lifting or pushing Walking on level surface at 6Km hr^{-1} while carrying a 3 Kg load
Heavy	Carpenter sawing by hand Shoving dry sand Heavy assembly work on a non-continuous basis Intermittent heavy lifting with pushing or pulling.

Table X. Mapping of sectors into labour intensity.

Heavy	Medium	Light
Rice	Wheat and other grains	Processed Food
Fruit and Vegetables	Oil Seeds	Minerals (nec)
Sugar	Cotton	Light Manufacturing
	Other crops	Transport and communication
	Livestock and meats	Services
	Dairy	
	Forestry	
	Coal	
	Oil	
	Gas	
	Heavy manufacturing	
	Utilities and construction	

Table X. Range of Shocks calculated from the CMIP5 Database for reduced labour capacity for the Historical Simulation of 2010.

	2010					
	Light Labour		Medium Labour		Heavy Labour	
Argentina	0.00	0.00	0.00	0.00	-0.18	0.00
Australia	0.00	0.00	0.00	0.00	-0.16	0.00
Bangladesh	-1.33	0.00	-5.71	0.00	-9.35	0.00
Brazil	0.00	0.00	0.00	0.00	-0.10	0.00
Canada	0.00	0.00	0.00	0.00	0.00	0.00
China	-0.01	0.00	-0.39	0.00	-2.07	0.00
Egypt	-0.02	0.00	-0.65	0.00	-2.70	0.00
EU27 and EFT	0.00	0.00	0.00	0.00	-0.03	0.00
Hong King	0.00	0.00	-1.03	0.00	-10.87	0.00
India	-5.70	0.00	-8.17	-0.02	-11.77	-2.53
Indonesia	0.00	0.00	0.00	0.00	0.00	0.00
Japan	0.00	0.00	0.00	0.00	-0.04	0.00
Korea	0.00	0.00	0.00	0.00	0.00	0.00
Mexico	0.00	0.00	-0.01	0.00	-1.10	0.00
Middle East	-3.26	0.00	-10.70	0.00	-14.10	-0.22
Nigeria	0.00	0.00	-4.48	0.00	-7.76	0.00
North Africa	0.00	0.00	0.00	0.00	-0.39	0.00
New Zealand	0.00	0.00	0.00	0.00	0.00	0.00
Pakistan	-8.19	0.00	-11.84	0.00	-15.35	-1.28
Philippines	0.00	0.00	-0.04	0.00	-5.20	0.00
Rest of EastAsia	0.00	0.00	-0.35	0.00	-2.60	0.00
REECCAsia	-0.43	0.00	-0.82	0.00	-1.17	0.00
Rest Latin America	0.00	0.00	0.00	0.00	-0.21	0.00
Rest SSA	-0.38	0.00	-0.81	0.00	-3.32	0.00
Rest of South Asia	-0.74	0.00	-3.55	0.00	-7.40	0.00
Russia	0.00	0.00	0.00	0.00	0.00	0.00
SSA	0.00	0.00	0.00	0.00	0.00	0.00
Thailand	0.00	0.00	-0.85	0.00	-8.01	0.00
USA	0.00	0.00	0.00	0.00	-0.39	0.00
Vietnam	-0.10	0.00	-3.17	0.00	-10.50	0.00

Table X. Range of Shocks calculated from the CMIP5 Database for reduced labour capacity for RCP2.6 for 2100.

	RCP 2.6					
	Light Labour		Medium Labour		Heavy Labour	
Argentina	0.00	0.00	-0.11	0.00	-1.08	0.00
Australia	0.00	0.00	-0.23	0.00	-3.00	0.00
Bangladesh	-3.27	0.00	-8.69	0.00	-18.89	-0.57
Brazil	0.00	0.00	-0.54	0.00	-6.18	0.00
Canada	0.00	0.00	0.00	0.00	0.00	0.00
China	-0.66	0.00	-2.96	0.00	-6.32	0.00
Egypt	-1.15	0.00	-3.85	0.00	-9.67	0.00
EU27 and EFT	0.00	0.00	-0.01	0.00	-0.24	0.00
Hong King	-2.41	0.00	-14.45	0.00	-29.30	0.00
India	-16.37.	0.00	-29.11	-0.09	-43.36	-5.59
Indonesia	0.00	0.00	0.00	0.00	-0.94	0.00
Japan	0.00	0.00	-2.62	0.00	-7.83	0.00
Korea	0.00	0.00	0.00	0.00	-0.02	0.00
Mexico	0.00	0.00	-1.36	0.00	-9.71	0.00
Middle East	-12.57	0.00	-27.13	0.00	-43.65	-0.87
Nigeria	-1.10	0.00	-10.65	0.00	-27.34	0.00
North Africa	0.00	0.00	-0.36	0.00	-5.10	0.00
New Zealand	0.00	0.00	0.00	0.00	0.00	0.00
Pakistan	-21.7	0.00	-33.52	-0.02	-45.73	-2.82
Philippines	-0.50	0.00	-7.03	0.00	-21.25	0.00
Rest of EastAsia	-0.62	0.00	-3.73	0.00	-9.85	0.00
REECCAsia	-0.99	0.00	-1.34	0.00	-3.28	-0.01
Rest Latin America	0.00	0.00	-0.04	0.00	-3.01	0.00
Rest SSA	-0.69	0.00	-3.44	0.00	-9.88	-0.02
Rest of South Asia	-3.69	0.00	-8.34	0.00	-14.70	-0.00
Russia	0.00	0.00	0.00	0.00	0.00	0.00
SSA	0.00	0.00	0.00	0.00	0.00	0.00
Thailand	-1.46	0.00	-14.66	0.00	-36.24	0.00
USA	-0.00	0.00	-0.53	0.00	-3.04	0.00
Vietnam	-5.31	0.00	-17.79	0.00	-36.87	0.00

Table X. Range of Shocks calculated from the CMIP5 Database for reduced labour capacity for RCP4.5 for 2100.

	RCP 4.5					
	Light Labour		Medium Labour		Heavy Labour	
Argentina	-0.13	0.00	-1.13	0.00	-3.34	0.00
Australia	-0.26	0.00	-1.91	0.00	-9.12	-0.01
Bangladesh	-9.44	0.00	-18.08	-0.01	-30.18	-1.57
Brazil	-0.71	0.00	-5.58	0.00	-16.83	0.00
Canada	0.00	0.00	0.00	0.00	0.00	0.00
China	-3.33	0.00	-7.03	0.00	-11.27	-0.10
Egypt	-3.59	0.00	-8.10	0.00	-22.21	0.00
EU27 and EFT	0.00	0.00	-0.166	0.00	-0.79	0.00
Hong Kong	-13.33	0.00	-28.86	0.00	-47.05	0.00
India	-27.69	-0.03	-41.69	-3.39	-56.52	-14.20
Indonesia	0.00	0.00	-0.68	0.00	-9.89	0.00
Japan	-1.76	0.00	-6.79	0.00	-13.56	0.00
Korea	0.00	0.00	0.00	0.00	-1.808	0.00
Mexico	-1.44	0.00	-10.51	0.00	-26.09	0.00
Middle East	-31.24	0.00	-48.30	0.00	-64.52	-4.06
Nigeria	-18.51	0.00	-31.36	-0.94	-46.23	-1.51
North Africa	-1.05	0.00	-7.02	0.00	-18.68	0.00
New Zealand	0.00	0.00	0.00	0.00	0.00	0.00
Pakistan	-36.36	-0.01	-48.81	-2.64	-60.35	-8.18
Philippines	-5.73	0.00	-18.48	0.00	-38.38	0.00
Rest of EastAsia	-3.84	0.00	-9.86	0.00	-18.40	-0.29
REECCAsia	-1.85	0.00	-4.60	-0.01	-8.70	-0.16
Rest Latin America	-0.05	0.00	-2.16	0.00	-11.73	0.00
Rest SSA	-3.63	0.00	-9.43	0.00	-18.09	-0.60
Rest of South Asia	-9.94	0.00	-17.29	-0.011	-27.32	-0.35
Russia	0.00	0.00	0.00	0.00	-0.01	0.00
SSA	0.00	0.00	0.00	0.00	0.00	0.00
Thailand	-15.88	0.00	-38.49	0.00	-56.54	-1.06
USA	-0.69	0.00	-3.38	0.00	-6.56	0.00
Vietnam	-16.18	0.00	-35.76	0.00	-54.48	-1.94

Table X. Range of Shocks calculated from the CMIP5 Database for reduced labour capacity for RCP6.0 for 2100.

	RCP 6.0					
	Light Labour		Medium Labour		Heavy Labour	
Argentina	-0.23	0.00	-1.40	0.00	-4.19	0.00
Australia	-0.29	0.00	-3.27	0.00	-13.56	-0.02
Bangladesh	-12.91	0.00	-24.33	-0.24	-36.50	-3.77
Brazil	-1.70	0.00	-9.62	0.00	-21.96	0.00
Canada	0.00	0.00	0.00	0.00	0.00	0.00
China	-4.00	0.00	-7.90	0.00	-12.40	-0.43
Egypt	-4.23	0.00	-10.86	0.00	-24.60	0.00
EU27 and EFT	0.00	0.00	-0.30	0.00	-1.73	0.00
Hong Kong	-16.26	0.00	-31.67	0.00	-50.28	-0.92
India	-33.32	-0.68	-48.40	-7.81	-62.69	-19.70
Indonesia	0.00	0.00	-0.82	0.00	-17.43	-0.04
Japan	-4.11	0.00	-10.61	0.00	-18.42	0.00
Korea	0.00	0.00	-0.13	0.00	-4.95	0.00
Mexico	-2.50	0.00	-13.42	0.00	-29.74	-0.19
Middle East	-24.72	-0.09	-39.03	-1.79	-54.80	-6.60
Nigeria	-24.45	0.00	-40.36	-0.42	-57.29	-5.25
North Africa	-2.48	0.00	-6.22	0.00	-16.76	0.00
New Zealand	0.00	0.00	0.00	0.00	0.00	0.00
Pakistan	-38.97	-0.35	-50.00	-5.20	-60.96	-10.97
Philippines	-9.67	0.00	-26.31	0.00	-46.57	-2.95
Rest of EastAsia	-4.20	0.00	-10.61	0.00	-19.48	-1.68
REECCAsia	-1.70	0.00	-2.63	-0.08	-5.11	-0.34
Rest Latin America	-0.96	0.00	-7.92	0.00	-19.96	-0.04
Rest SSA	-7.13	0.00	-14.57	-0.10	-24.92	-1.87
Rest of South Asia	-5.54	0.00	-11.45	-0.11	-20.58	-1.47
Russia	0.00	0.00	0.00	0.00	0.00	0.00
SSA	0.00	0.00	0.00	0.00	-0.39	0.00
Thailand	-16.64	0.00	-39.04	0.00	-57.04	-7.21
USA	-0.98	0.00	-3.80	0.00	-6.96	0.00
Vietnam	-18.55	0.00	-38.86	0.00	-57.12	-7.52

Table X. Range of Shocks calculated from the CMIP5 Database for reduced labour capacity for RCP8.5 for 2100.

	RCP 8.5					
	Light Labour		Medium Labour		Heavy Labour	
Argentina	-9.47	0.00	-14.72	0.00	-20.75	-0.14
Australia	-11.91	0.00	-22.97	-0.24	-34.37	-6.19
Bangladesh	-35.62	0.00	-48.79	-1.83	-62.91	-7.39
Brazil	-27.04	0.00	-43.56	-0.15	-60.53	-5.70
Canada	-0.21	0.00	-0.66	0.00	-1.38	0.00
China	-14.58	0.00	-22.69	-0.33	-34.04	-1.89
Egypt	-46.19	0.00	-60.88	0.00	-76.64	-0.04
EU27 and EFT	-2.67	0.00	-5.52	0.00	-9.73	0.00
Hong Kong	-46.13	0.00	-64.61	-0.07	-79.91	-5.42
India	-61.19	-7.99	-75.38	-20.62	-87.84	-35.60
Indonesia	-8.88	0.00	-32.46	0.00	-51.32	-4.00
Japan	-16.02	0.00	-25.97	0.00	-35.55	0.00
Korea	-2.55	0.00	-15.48	0.00	-33.15	0.00
Mexico	-26.21	0.00	-44.86	-0.21	-60.69	-3.52
Middle East	-82.21	-2.40	-86.60	-7.93	-87.26	-15.85
Nigeria	-65.55	-0.89	-81.78	-5.17	-90.69	-19.04
North Africa	-39.57	0.00	-53.47	-0.01	-67.03	-0.16
New Zealand	0.00	0.00	0.00	0.00	0.00	0.00
Pakistan	-71.82	-5.71	-84.79	-11.87	-90.99	-18.24
Philippines	-36.31	0.00	-55.91	0.00	-72.00	-8.84
Rest of EastAsia	-18.02	0.00	-28.26	-1.02	-41.55	-7.35
REECCAsia	-16.87	-0.11	-25.29	-0.40	-35.15	-0.79
Rest Latin America	-15.95	0.00	-29.56	-0.11	-42.70	-4.21
Rest SSA	-23.45	-0.30	-39.06	-2.53	-56.37	-7.73
Rest of South Asia	-41.91	-0.10	-54.61	-1.19	-67.31	-4.48
Russia	-0.07	0.00	-0.25	0.00	-0.66	0.00
SSA	-0.61	0.00	-6.78	0.00	-18.00	0.00
Thailand	-58.47	0.00	-75.08	-4.06	-89.29	-22.25
USA	-6.54	0.00	-11.64	0.00	-17.26	-0.34
Vietnam	-54.40	0.00	-71.52	-5.37	-86.08	-25.43